Synthesis and Characterization of Biocompatible Polymer Interlayers on Titanium Implant Materials

Nina Adden,[†] Lara J. Gamble,[‡] David G. Castner,[‡] Andrea Hoffmann,[§] Gerhard Gross,[§] and Henning Menzel*[,†]

Institut für Technische Chemie, Abt. TC Makromolekularer Stoffe, Technische Universität Braunschweig, Hans-Sommer-Strasse 10, 38106 Braunschweig, Germany, National ESCA and Surface Analysis Center for Biomedical Problems, Departments of Bioengineering and Chemical Engineering, Box 351750, University of Washington, Seattle, WA 98195, and Department of Gene Regulation and Differentiation, Gesellschaft für Biotechnologische Forschung, 38124 Braunschweig, Germany

Received May 15, 2006; Revised Manuscript Received July 7, 2006

A bifunctional copolymer series of (4-vinylbenzyl)phosphonic acid diethylester and *N*-acryloxysuccinimide was developed as an interlayer with the aim of immobilizing proteins on titanium surfaces. Copolymers with varying compositions were synthesized, and an alternating copolymerization of the two monomers was found. The copolymers form ultrathin films of about 2−8 nm on titanium surfaces in a simple dipping process, as estimated from the attenuation of the titanium X-ray photoelectron spectroscopy (Ti-XPS) signal. The films were characterized by infrared spectroscopy, XPS, and time-of-flight secondary ion mass spectrometry. The results indicate that the immobilization is due to phosphonate groups, and thus the phosphonate content of the copolymers is decisive for the final film thickness. These polymer films were examined for their potential protein binding capacity by using trifluoroethylamine derivatization and subsequent XPS analysis as a reactivity assay.

Introduction

Functionalization of implant materials with signaling proteins is a promising approach for many medical problems. For example, it has been shown that bone morphogenetic proteins (BMPs) influence bone formation positively,[1−3] making them interesting for clinical use for orthopedic and dental implants. The fast transport of the such proteins from the site of application necessitates controlled delivery systems.[1,4] A variety of delivery systems, for example, collagen,[5] porous hydroxyapatite scaffolds,[6] or polymeric systems such as poly(lactid-*co*-glycolic acid),[4] methacrylate systems,[7] and a thermoreversible polymer,[8] have been studied for bone tissue engineering applications. Few studies exist in which BMPs are covalently bound to the metal implant surface for orthopedic or dental implants.[9,10] Such implant surfaces are the ideal places of delivery for these applications, because a direct bone implant contact is desired. Initial experiments with surface-immobilized BMP-2 have shown that covalent immobilization does not interfere with the biological activity of BMP-2,[11] and, furthermore, the protein in its immobilized form increased the metal bone contact and is more efficient than soluble BMP-2 doses.[11,12]

The classical immobilization schemes for bioactive substances on titanium involve silane monolayers[9,13,14] or, developed more recently, phosphonic acid monolayers.[15−17] These approaches include several modification steps, and the silane layers may be hydrolyzed under physiological conditions.[18−20] For example, Jennissen et al. first pretreated the titanium surface with chromosulfuric acid for silanization with (3-aminopropyl)-triethoxysilane. This amine-terminated surface was activated with carbonyldiimidazole before coupling BMP to the surface.[9] In comparison, Puelo et al. plasma polymerized allylamine to titanium surfaces and coupled the protein with carbodiimide and *N*-hydroxysuccinimide in a one- or two-step procedure.[10] Only the two-step scheme produced a surface in which the protein retained its biological activity. Other peptide immobilization schemes exist, as seen in Tosatti et al., where RGD peptide was immobilized to titanium surfaces using a poly(L-lysine) poly(ethylene glycol) graft copolymer prefunctionalized with the peptide. The polymer was immobilized via electrostatic interactions of the positively charged amino groups with the negatively charged TiO_2.[21] Unlike RGD, which can be coupled to poly(L-lysine-*graft*-ethylene glycol) via a cysteine group,[21] BMP-2 does not have any available cysteines.[1,9] BMP-2 and other proteins are often coupled via their amine functionalities through an *N*-acryloxysuccinimide (NASI) linker.[8,22] For example, with drug delivery polymers, these amines are used to couple BMP-2 while retaining its activity.[8] Furthermore, we have already successfully employed an *N*-hydroxysuccinimide ester-functionalized self-assembled monolayer to couple BMP-2 to titanium surfaces.[17]

An ideal, simple, and effective immobilization method could be based on a polymer that is able to couple to titanium, provides a biocompatible surface, and can simultaneously couple proteins. In an earlier study, we characterized different polymer surfaces regarding their ability to support the adhesion and proliferation of murine mesenchymal precursor stem cells (BMP2−C3H10T1/2). These cells possess osteoblastic characteristics in vitro and can be considered as a good model system for the assessment of osteoblast−polymer interactions and for the prediction of in vivo behavior with respect to the probability of enhanced osseointegration.[23] One of the best surfaces in this study was poly(4-vinylbenzyl)phosphonic acid diethylester (p(VBP)). This polymer should be able to couple to the titanium surface via its phosphonate group. Guerrero et al. reported that, besides the

* Corresponding author. E-mail address: h.menzel@tu-braunschweig.de. Tel: ++49-531-391-5361. Fax ++49-531-391-5357.
[†] Technische Universität Braunschweig.
[‡] University of Washington.
[§] Gesellschaft für Biotechnologische Forschung.

10.1021/bm060473j CCC: $33.50
Published on Web 08/25/2006

known phosphonic acid molecules, phosphonic esters could be used to couple to metal oxide surfaces.[24] However, to the best of our knowledge, no reports exist using the phosphonic ester group to couple polymers to titanium surfaces.

In this study, we describe a copolymer system of (4-vinylbenzyl)phosphonic acid diethylester (VBP) and NASI, which should be able to both attach to titanium surfaces and bind proteins such as, for example, BMP-2. The aim of this study was to determine the copolymerization parameters of the two monomers and to examine the ability of the resulting copolymers to attach to titanium. This was examined by infrared spectroscopy, X-ray photoelectron spectroscopy (XPS), and time-of-flight secondary ion mass spectrometry (ToF-SIMS). Furthermore, the principal ability to couple molecules via amine groups was tested using trifluoroethylamine (TFEA) derivatization and XPS analysis.

Materials and Methods

Materials. All solvents were dried and distilled using standard procedures.[25] 2,6-di-*tert*-butyl-4-methylphenol (Aldrich), azobisisobutyronitrile (AIBN, Acros), and NASI (Acros) were used as received. Vinylbenzyl chloride (Acros) was dried over calcium hydride and distilled under reduced pressure. Triethyl phosphite (Fluka) was dried over sodium and distilled under reduced pressure. VBP was synthesized according to the literature.[26,27]

Squares of Ti90/Al6/V4 (25×25 mm^2, 1 mm thick) (Goodfellow) were cut into 10×10 mm^2 pieces and polished as previously reported.[28] Subsequently, they were rinsed and sonicated with dichloromethane, acetone, and methanol, dried in a stream of nitrogen, and stored in an oven at 120 °C. Before use, the substrates were sonicated in 5% RBS-35 detergent solution (Pierce), three times in Millipore water, twice in acetone, and twice in methanol for 10 min each; they were then dried in a stream of nitrogen.

Polymerization Reactions. p(VBP) was synthesized by radical polymerization in tetrahydrofuran (THF) at 60 °C using AIBN as the initiator. Copolymerizations were carried out using 1 M solutions of VBP and NASI in THF. 1 mol % AIBN was used as the initiator, and the reaction time was limited to 60 min to ensure low conversions. Nine different ratios of the monomers were tested. The experiment was repeated three times. The polymers were characterized by gel permeation chromatography, NMR, and elemental analysis. The composition was calculated using the C/N ratio of the elemental analysis.

Immobilization of Polymers onto Ti-6Al-4V Surfaces. A solution of the polymer (10 mg/mL) was spin coated onto the titanium squares at a speed of 2000 rpm for 30 s. The solvents were dry THF, a mixture of chloroform and THF, or chloroform for higher succinimide contents of the polymers. The squares were heated in an oven at 120 °C for 18 h and then rinsed six times for 20 min with sonication in the respective solvents.

Reactivity Test of the Activated Polymer Films. The activity of the surfaces was tested according to ref 29 using TFEA as a probe. The activated samples were immersed in a 0.17 M solution of TFEA in THF under shaking for 15 h at room temperature. After removal from solution, they were washed twice for 15 min in THF under shaking, and 15 min in THF and 5 min in Millipore water under sonication. They were dried in a stream of nitrogen.

NMR and Fourier Transform Infrared (FTIR) Characterization. ^{1}H NMR measurements were conducted on a Bruker AM400 spectrometer (400 MHz). Sample concentrations were 60−80 mg/mL. Infrared spectra of the polymer films were obtained with a Bruker IFS 120 FTIR spectrometer using a mercury cadmium telluride detector. Spectra were collected with a GIR accessory (Bruker A518) with 2048 scans, and the resolution was 4 cm^{-1}. Unmodified titanium squares were used as a reference sample.

Elemental Analysis. The CHN content of the copolymers was determined using a Thermo Quest CE Instruments Flash EA 1112. The composition of the copolymers was calculated using the C/N ratio (see Supporting Information).

Size Exclusion Chromatography (SEC). Molecular weights and molecular weight distributions were measured by SEC in dimethylformamide (DMF; membrane filtered and degassed) containing LiBr (0.1 mol %) on two PL-gel 5 μm mixed-C columns (Polymer Laboratories) at 80 °C and a flow rate of 0.5 mL/ min. Detection was performed with a Melz LCD201 differential refractive-index detector (set at 35 °C), a Thermo Separation Products UV150 Spectraseries UV−visible light detector set at 270 nm, and a TriStar MiniDawn light scattering detector from Wyatt Technology (angles at 30, 90, and 120°) using the ASTRA software (Wyatt Technologies).

Ellipsometry. Film thicknesses were determined using a multiskop (Optrel) in the ellipsometry mode. Each square was measured as a reference before treatment.

XPS Analysis. XPS measurements were obtained using a Kratos AXIS Ultra DLD instrument equipped with a monochromatized Al Kα X-ray source. Compositional survey and detail scans (P2p, C1s, N1s, O1s, and F1s) were acquired using a pass energy of 80 eV. High-resolution spectra (C1s and O1s) were obtained using a pass energy of 20 eV. All spectra were taken at a 0° takeoff-angle. (Takeoff-angle is defined as the angle of the analyzer lens with respect to the surface normal.) For the high-resolution spectra, peak binding energies were referenced to the C1s (C−C/C−H) peak at 285.0 eV. Three spots on two or more replicates of each sample were analyzed. The compositional data are averages of the values determined at each spot. Data analysis was performed on Vision2 software.

ToF-SIMS Analysis. ToF-SIMS spectra were acquired on a Physical Electronics PHI 7200 time-of flight spectrometer using an 8 keV Cs^+ primary ion source in the pulsed mode. Spectra were acquired for both positive and negative secondary ions over a mass range of (m/z) 0−1000. The area of analysis for each spectrum was 100×100 μm, and the total ion dose was maintained below 1×10^{12} ions/cm^2. The mass resolutions ($m/\Delta m$) were typically 6000 for the positive ions at the $m/z = 27$ ($C_2H_3^+$) peak and 8000 for the negative spectra at $m/z = 25$ (C_2H^-). Three spots on two replicates of each sample were examined. Positive ion spectra were calibrated using the CH_3^+,$C_2H_3^+$, $C_3H_5^+$, and $C_6H_9^+$ peaks, and negative ion spectra were calibrated using the CH^-, C_2H^-, OH^-, and PO_3^- peaks. Calibration errors were kept below 10 ppm.

Principal Component Analysis (PCA). PCA reduces a multidimensional data set to new variables, called principal components (PCs). The PCs are linear combinations of the original variables in the data set. Scores show the relationship between different samples on each PC. The loadings relate the original variables, in our case, the ToF-SIMS peaks, to the scores and describe which variables are responsible for the differences seen between the samples. For a given PC, it generally can be said that variables with positive loadings typically correspond to samples with positive scores.

Prior to multivariate analysis, a peak list was created that contained all peaks with intensities above about 40 counts. The peak areas for each spectrum were calculated and normalized to the total intensity of each respective spectrum. Finally, the data were mean centered to ensure that the variance in the data set was due to differences in sample variances rather than differences in sample means. PCA was performed using the PLS Toolbox v. 2.0 (Eigenvector Research, Manson, WA) for MATLAB (Mathworks, Inc., Natick, MA). The 95% confidence limits for the score plots were calculated using the methods described by Wagner et al.[30] For a detailed description of PCA, see references 30 and 31.

Results and Discussion

Our approach for a new and easy applicable method to immobilize proteins to titanium implant surfaces is to use a

Scheme 1. Copolymerization of VBP and NASI and Suggested Reactions with a Titanium Surface and a Protein, Respectively

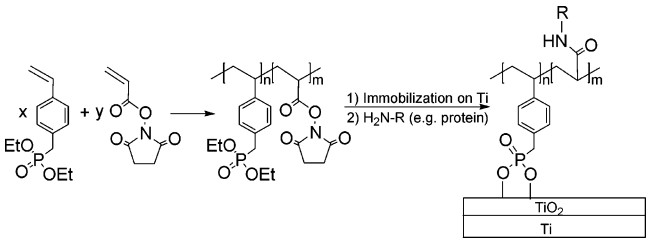

copolymer that is able to bind to the surface as well as to couple proteins. This copolymer consists of VBP, which allows binding to titanium via its phosphonate groups, and NASI, having active ester groups commonly used for protein coupling (see Scheme 1).

Copolymerization of VBP and NASI. The two monomers were copolymerized in THF using free-radical polymerization methods. The reaction time was kept short, minimizing conversion, so the copolymerization parameters could be determined. The resulting copolymers were characterized by SEC, NMR, and elemental analysis. SEC measurements were performed with DMF containing LiBr as an eluent. All polymers have a monomodal distribution with a typical polydispersity of 1.7−2.2. The molecular weights (M_n) are about 60−90 000 g/mol for most polymers. Polymers with the highest NASI content have molecular weights of about 20 000 g/mol, and polymers with the highest VBP content have molecular weights of about 140 000 g/mol (see Supporting Information). Artifacts due to reactions of the NASI contents of the polymers with the decomposition products of DMF used as eluent cannot be excluded.

A typical NMR of a copolymer is shown in Figure 1. From the integrals of the different NMR peaks, the ratio of the monomers in the copolymer can be calculated. These calculated values correspond to the composition calculated from the C/N ratio of the elemental analysis. The elemental analysis was used to calculate the composition of all copolymers because the NMR integral h_2 sometimes included a water signal from the solvent ($CDCl_3$ or DMSO-d_6), resulting in an overestimation of the NASI content. These copolymer compositions are plotted against the monomer feed compositions to give the copolymerization diagram (Figure 2).

As seen in Figure 2, the azeotropic point is at 0.5, typical of monomers forming a nearly perfect alternating copolymer. This indicates that one monomer type is more likely to react with the other monomer type than with itself. The copolymerization parameters r_1 and r_2 should be close to zero. Indeed, copolymerization parameters of $r_1 = 0.16$ for VBP and $r_2 = 0.13$ for NASI were obtained using the method of Kelen and Tüdös (see Supporting Information). The r parameters give clear evidence that copolymers are obtained in which the different monomers are distributed homogeneously along the polymer chain.

For further experiments, five different compositions of the copolymer p(VBP-*co*-NASI) (**A**−**E**) and the homopolymer p(VBP) (**H**) were studied (see Table 1).

Preparation of Thin Polymer Layers on Ti90/Al6/V4. As implant material, we chose a titanium alloy (90% Ti, 6% Al, and 4% V), which, because of its superior mechanical properties, is used more often for orthopedic implants than pure titanium. As common for pure titanium and titanium rich alloys, the surface is covered with a stable titanium oxide layer. The polymers were applied to the Ti90/Al6/V4 squares (10 × 10 × 1 mm) by spin coating (or dipping) from solution. The samples

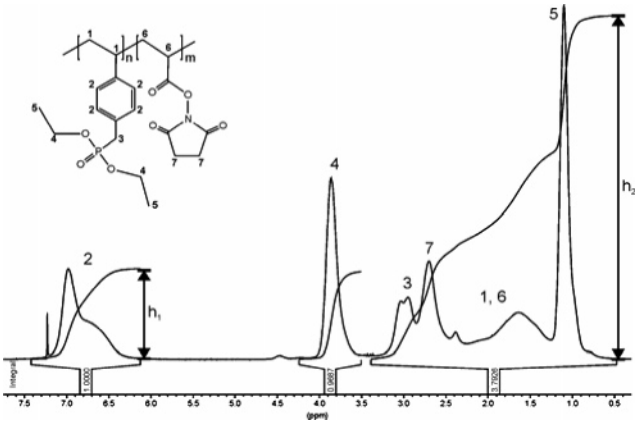

Figure 1. NMR of p(VBP-*co*-NASI) in $CDCl_3$.

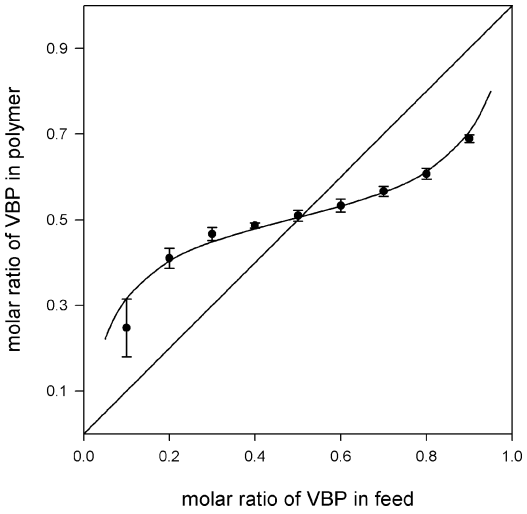

Figure 2. Copolymerization diagram of vinylbenzylphosphonate with NASI (the curve is calculated using the r parameter determined by the Kelen−Tüdös method).

Table 1. Compositions of Copolymers Used for Further Experiments as Determined by Elemental Analysis

polymer		ratio VBP	ratio NASI
p(VBP)	**H**	1.00	0.00
p(VBP-*co*-NASI)	**A**	0.70	0.30
p(VBP-*co*-NASI)	**B**	0.62	0.38
p(VBP-*co*-NASI)	**C**	0.53	0.47
p(VBP-*co*-NASI)	**D**	0.43	0.57
p(VBP-*co*-NASI)	**E**	0.32	0.68

were annealed at 120 °C overnight to enhance cleavage of the P−OEt groups and improve the coupling to the surface.[24] After the heating process, the samples were washed thoroughly with an appropriate solvent (THF or chloroform) to remove excess polymer. Even after extreme washing conditions (six times for 30 min) in ultrasonic bath (THF), 20 h Soxhlet extraction (THF), and 2 h ultrasonic bath, a p(VBP) film with a thickness of about 8 nm, as measured by ellipsometry, remained on the surface. Because the film thickness had become constant after the six washes in the ultrasonic bath and was not further reduced by the Soxhlet extraction, only the ultrasonic washes were used for all remaining samples.

Grazing incidence FTIR spectra of p(VBP)- and p(VBP-*co*-NASI)-treated surfaces were recorded with an untreated titanium surface as a reference. Main bands of the polymers are found in the spectra of the thin films on titanium, as can be seen in Figure 3 by comparing the thin film spectra with the bulk

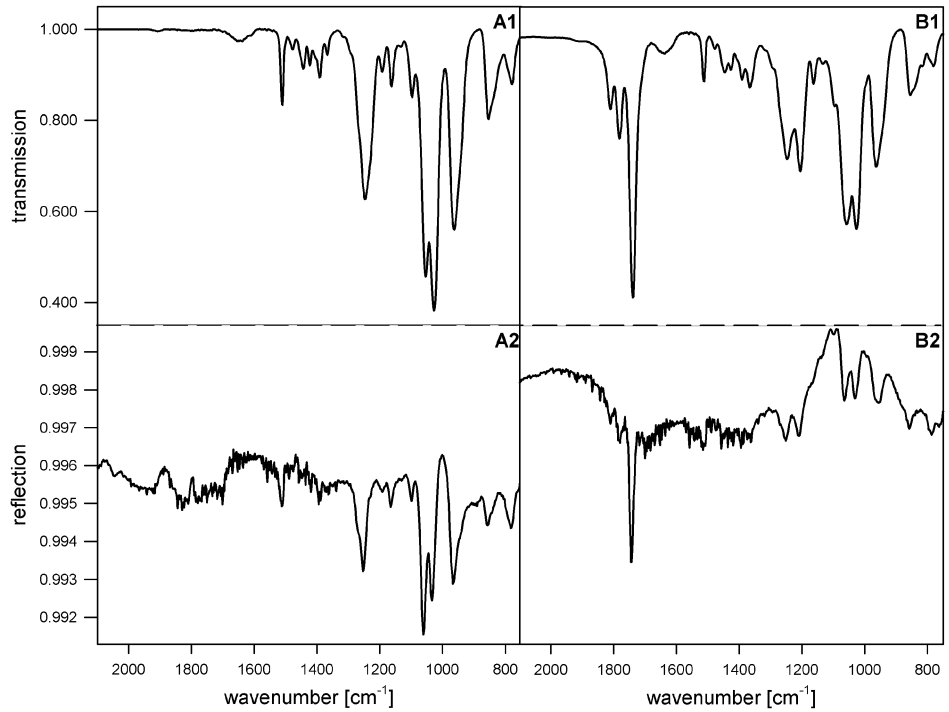

Figure 3. Infrared spectra of (A1) p(VBP) in a KBr pellet, (A2) a p(VBP) thin film on Ti90/Al6/V4, (B1) p(VBP-*co*-NASI) in a KBr pellet, and (B2) a p(VBP-*co*-NASI) thin film on Ti90/Al6/V4.

polymer spectra. The main signals found for the VBP (**A1** and **A2**) are the P═O stretching vibration at 1247 cm^{-1}, the P−O−C (aliphatic) adsorption bands at 1057 and 1027 cm^{-1}, and the band found at 963 cm^{-1}, characteristic for the P^V−O vibration.[32] The copolymers p(VBP-*co*-NASI) (**B1** and **B2**) have an additional band at 1739 cm^{-1} for the carbonyl groups and at 1205 cm^{-1} from the C−O stretching vibration. Upon immobilization onto titanium, the band at 1027 cm^{-1} (P−OEt) decreases relative to the band at 1057 cm^{-1}, possibly because of the cleavage of some P−OEt groups upon coupling to the surface, as has been suggested by Guerrero et al. as the binding mechanism for phosphonic acid esters.[24]

XPS measurements were performed on all copolymer p(VBP-*co*-NASI) (**A**−**E**) films and the homopolymer p(VBP) (**H**) film. The polished Ti90/Al6/V4 substrate was measured as a reference. Besides the expected Ti (21.4 ± 0.4%) and O (57.4 ± 1.4%) components from Ti90/Al6/V4, hydrocarbon contamination (20.4 ± 1.5%) along with N (0.5 ± 0.1%), P (0.2 ± 0.1%), and sometimes Pb contaminants were detected. These results are in agreement with literature data for polished and solvent-cleaned titanium samples.[33−35] This degree of contamination is expected to be low enough that it should not interfere with the subsequent modification steps. The XPS-determined elemental compositions for the different polymer films along with the substrate composition are shown in Table 2.

Compared to the bare titanium substrate, the XPS results for the p(VBP) film showed an increase in carbon and phosphorus signals from the polymer with a decrease in the substrate signals from the titanium substrate (titanium and oxygen) and the contamination signal (nitrogen). Compared to the bare titanium substrate, the p(VBP-*co*-NASI) films showed an increase in the carbon, phosphorus, and nitrogen signals, with a decrease in the Ti and O signals. From the attenuation of the Ti signal, a film thickness of 8−2 nm can be estimated. With decreasing VBP content in the copolymers, the carbon and phosphorus signals decreased, and the oxygen, nitrogen, and titanium signals increased. The decrease of the phosphorus and increase of the nitrogen signals corresponds to the decreased amount of VBP in the copolymer composition. The overall decrease of C and increase in O and Ti indicates a decreasing film thickness with decreasing VBP content of the polymer. This is consistent with the involvement of the phosphonate group in the attachment of the copolymers to the titanium surface. It is interesting to compare the surface P/N ratio measured by XPS (P/N (XPS)) to the bulk P/N ratio measured by elemental analysis results (P/N (E/A)) (see Table 3).

As expected, the P/N ratio decreased with decreasing VBP content of the copolymer. However, for all of the samples, the XPS P/N ratio is lower than the elemental analysis P/N ratio. This result was unexpected since the hydroxysuccinimide (NHS) group of the NASI component is unstable toward hydrolysis, and nitrogen loss during the immobilization process seems more

Table 2. XPS-Determined Elemental Compositions of the p(VBP) (**H**) Film, the p(VBP-*co*-NASI) (**A**−**E**) Films, and the Polished Ti90/Al6/V4 Substrate

	atomic concentration [%]				
polymer	C1s	O1s	P2p	N1s	Ti2p
substrate	20.4 ± 1.5	57.4 ± 1.4	0.2 ± 0.1	0.5 ± 0.1	21.4 ± 0.4
H	79.3 ± 1.4	16.4 ± 0.8	4.0 ± 0.4	0.1 ± 0.0	0.4 ± 0.1
A	68.5 ± 3.5	24.2 ± 2.3	2.4 ± 0.2	1.7 ± 0.1	3.0 ± 1.1
B	65.8 ± 0.8	26.1 ± 0.8	2.2 ± 0.3	2.2 ± 0.1	3.6 ± 0.6
C	63.1 ± 3.6	28.2 ± 2.4	2.0 ± 0.3	2.5 ± 0.3	4.1 ± 1.0
D	53.0 ± 1.6	35.1 ± 1.0	1.4 ± 0.1	2.9 ± 0.1	7.2 ± 0.3
E	44.5 ± 3.6	41.3 ± 2.6	0.9 ± 0.1	2.8 ± 0.5	10.4 ± 1.2

Table 3. P/N Ratio of Copolymer Films

polymer	P/N (XPS)	P/N (E/A)
A	1.42	2.25
B	1.04	1.64
C	0.79	1.13
D	0.46	0.75
E	0.34	0.48

Table 4. Relative Peak Concentrations for the High-Resolution XPS C1s Spectra of the Polymer Thin Films (**H**, **A**−**E**)[a]

	XPS C1s peak concentrations [%](calculated value)		
polymer	**a** (285.0 eV)	**b** (286.0−287.0 eV)	**c** (289.0−289.2 eV)
H	80.7 ± 0.7 (84.6)	19.3 ± 0.7 (15.4)	
A	70.3 ± 0.4 (71.2)	22.2 ± 0.6 (20.6)	7.5 ± 0.5 (8.2)
B	67.6 ± 1.9 (67.2)	22.7 ± 1.9 (22.2)	9.7 ± 0.1(10.6)
C	62.7 ± 3.6 (61.8)	23.8 ± 4.0 (24.3)	13.5 ± 0.5 (13.9)
D	51.1 ± 3.9 (55.4)	31.1 ± 4.1 (26.8)	16.8 ± 0.2 (17.8)
E	52.3 ± 3.6 (47.0)	26.6 ± 3.3 (30.1)	21.1 ± 0.4 (22.9)

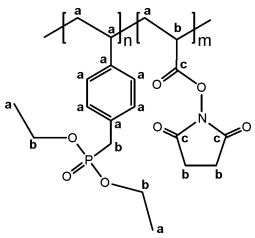

[a] Expected values calculated from the elemental analysis results are shown in parentheses.

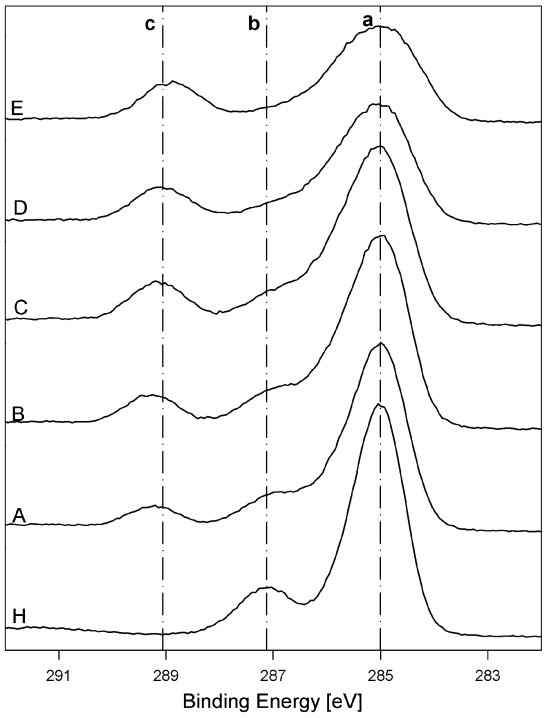

Figure 4. High-resolution XPS C1s spectra of p(VBP) (**H**) and p(VBP-*co*-NASI) (**A**−**E**) thin films on Ti90/Al6/V4.

probable.[36] The low surface phosphorus concentration may be due to an orientation of the VBP component of the copolymers to the titanium/polymer interface to reduce the surface energy and maximize polymer−titanium bonding. In such a configuration, the phosphorus XPS signal would be attenuated by the overlying polymer.

High-resolution C1s XPS measurements give further insight into the composition and structure of the polymer films. The spectra of the different copolymer films in comparison to the homopolymer film are shown in Figure 4.

The spectra of the copolymer films (**A**−**E**) show an additional peak near 289 eV compared to the p(VBP) film control (**H**). The 289 eV binding energy is typical for the carbonyl groups of the NHS ester.[37,38] In general, this peak (**c**) increases with increasing NASI content of the copolymer, while the peak at about 286.5 eV (attributed to the C−O bonds in the VBP) (**b**) decreases. The detailed assignments and peak concentrations for the different films are shown in Table 4.

The theoretical values given in parentheses were calculated according to the assignments given in the table using the compositions from the elemental analysis. The major peak (**a**) at 285.0 eV was assigned to the hydrocarbon of the polymer backbone and of the phenyl ring of the VBP. Thus, this peak is found to decrease with decreasing VBP content. The second peak near 286.5 eV (**b**) was attributed to the P−O−C groups, the P−C groups, and to the β-shifted carbon next to the carbonyl groups. The P−O−C and P−C groups are reported in the literature to have binding energies of 286.8 and 286.4 eV, respectively.[33,39] The β-shifted carbon is expected to have a binding energy of 285.7 eV.[40] Therefore, peak **b** shifts from 287 to 286 eV with decreasing VBP and increasing NASI content. Peak **c** from the carbonyl group of the NHS ester increases with increasing NASI content, as expected.[37,38] The relative concentration of peak **c** is always slightly lower than the theoretical value, possibly because of the hydrolysis of some NHS groups.[36] The values for copolymer **E** show slightly more hydrocarbon than predicted from the theoretical values. This polymer has the smallest film thickness, and it is likely that substrate hydrocarbon contamination may contribute to the carbon signal. Overall, the values correlate well with theory, indicating that the polymer films form with the NHS and phosphate active groups intact. Because the ethyl groups contribute to both peak **a** and peak **b**, and the hydrolysis of ester groups should not be extensive, the elemental composition as determined by XPS cannot give any evidence of whether the binding mechanism as suggested by Guerrero et al. is correct.[24]

ToF-SIMS measurements are more surface sensitive than XPS measurements. For molecular fragments, only the outer ~2 nm of the surface contributes to the spectra, providing a more accurate determination of which functional groups in the copolymer will be available to bind the protein. The NHS groups need to be present at the outer surface of the polymer to couple BMP-2. While XPS results indicate that the NHS groups are present, they may be entrapped in the polymer film or possibly already hydrolyzed.

ToF-SIMS of a reference titanium substrate showed primarily titanium peaks such as Ti^+, TiO^+, and TiO_2H^+ in the positive ion spectrum as well as common hydrocarbon contamination peaks such as the series $C_nH_{2n+1}^+$ and $C_nH_{2n-1}^+$. The negative ion spectrum was dominated by the O^- and OH^- peaks, but some phosphorus contamination peaks (PO_2^- and PO_3^-) were also detected. A few minor contaminants such as F^- and Cl^- were observed by ToF-SIMS that were not detected by XPS. The titanium ToF-SIMS results agree well with data in the literature.[33−35]

ToF-SIMS spectra of the different polymer films were compared by PCA. This simplifies data analysis, because it allows comparison of multiple spectra containing multiple peaks to determine which peaks vary the most within the data set. The PC1 scores for the negative-ion spectra are shown in Figure 5. PC 1 captures 88% of the variation in these spectra.

The PC1 scores show that surfaces coated with the homopolymer p(VBP) (**H**) are clearly separated from the surfaces

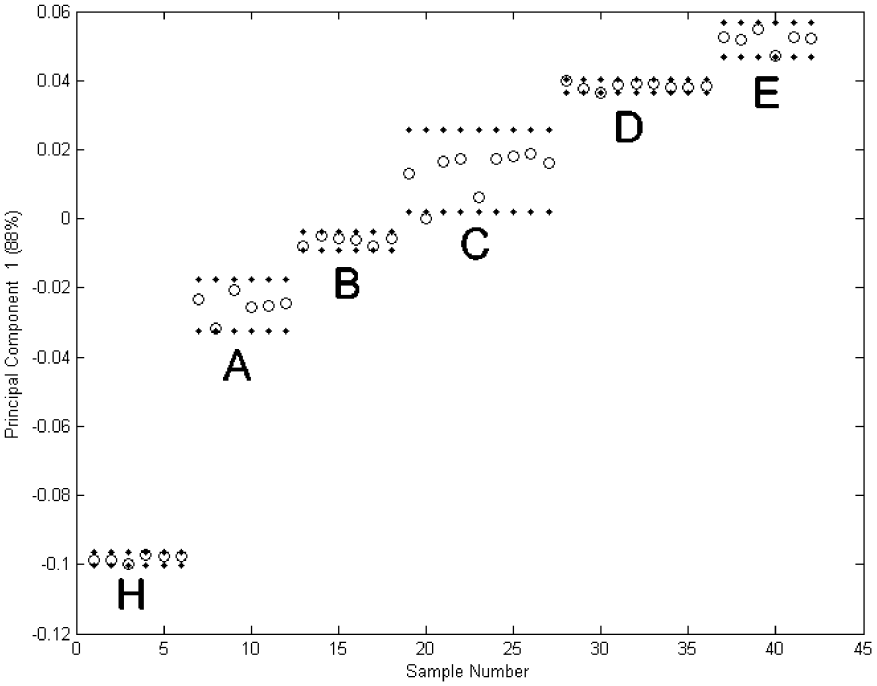

Figure 5. PC1 scores plot of the negative secondary ion spectra from the p(VBP) (**H**) film and the p(VBP-*co*-NASI) (**A**−**E**) films.

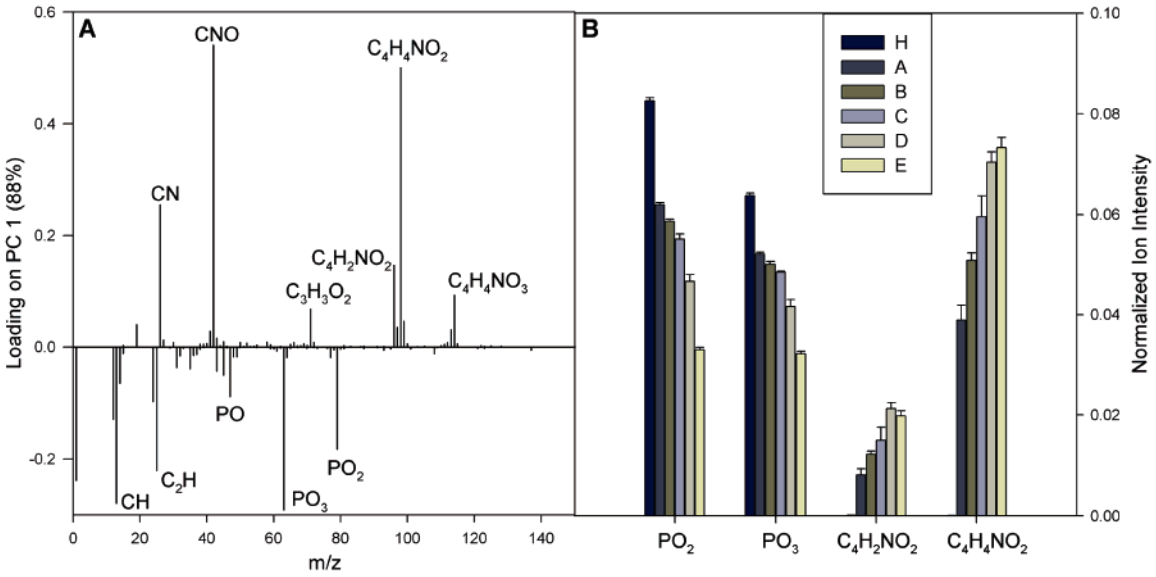

Figure 6. (A) PC1 loadings plot for the negative secondary ion spectra showing peaks responsible for the sample separation. (B) Comparison of some key molecular fragments from the different polymer films (normalized to the total ion yield of the spectrum).

coated with the copolymers p(VBP-*co*-NASI) (**A**−**E**). The copolymer surfaces of each different composition are also clearly separated from each other. The corresponding PC1 loadings plot (Figure 6A) shows the ToF-SIMS peaks responsible for this separation.

The positive loaded peaks can be correlated with the NASI content of the copolymers as these peaks correspond to the nitrogen content of the samples (CN^- and CNO^-), fragments from the NHS group ($C_4H_2NO_2^-$, $C_4H_4NO_2^-$, and $C_4H_4NO_3^-$), and by fragments from the acrylic acid group ($C_3H_3O_2^-$). The negative loaded peaks are predominantly phosphate-related peaks that correspond to the VBP content. The normalized ion intensities for some molecular fragments are shown in Figure 6B. The PO_2^- and PO_3^- peaks from VBP decrease with decreasing VBP content, while NHS group fragments $C_4H_2NO_2^-$ and $C_4H_4NO_2^-$ increase with increasing NASI content. The presence of these NHS group fragments indicate that some of NHS−ester groups remain intact and near the polymer surface.

The PC1 for the positive-ion spectra captures 77% of the variation in the dataset and clearly separates the different samples from each other (see Supporting Information). This separation is mainly due to positively loaded hydrocarbon fragments ($C_3H_7^+$, $C_4H_7^+$, and $C_5H_9^+$) and negatively loaded $H_2PO_2^-$, $H_2PO_3^-$, $C_7H_7^-$, and $C_9H_9^-$ peaks (see Supporting Info). The negatively loaded peaks are from the VBP portion of the copolymer, and their normalized intensities decrease with decreasing VBP content. The positive loaded peaks correlate with increasing NASI content. However, these fragments are not unique to the NASI monomer and suggest increasing hydrocarbon contamination with increasing NASI content, possibly due to decreasing film thickness.

Reactivity Assay of the Polymer Layers. After the successful immobilization of the polymers to the Ti90/Al6/V4

Table 5. XPS-Determined Elemental Composition of the Polymer Films after Reaction with TFEA[a]

	XPS concentration without TiO_2 [%]				
polymer	C	O	P	N	F
H	80.8 ± 0.3	15.6 ± 0.2	3.6 ± 0.1		
A	75.2 ± 1.0	20.3 ± 0.9	2.4 ± 0.1	1.9 ± 0.1	0.1 ± 0.1
B	73.8 ± 0.6	21.4 ± 0.6	2.1 ± 0.1	2.5 ± 0.1	0.1 ± 0.0
C	72.1 ± 0.7	22.7 ± 0.9	1.9 ± 0.1	3.0 ± 0.3	0.2 ± 0.1
D	68.1 ± 0.5	25.9 ± 0.6	1.5 ± 0.1	3.9 ± 0.1	0.5 ± 0.1
E	64.3 ± 1.4	29.0 ± 1.4	1.1 ± 0.1	4.5 ± 0.2	1.0 ± 0.3

[a] The TiO_2 substrate peaks have been subtracted, and the compositions have been renormalized to 100%.

surface, the reactivity of the NHS groups toward primary amino groups was tested. Samples coated with the different copolymers p(VBP-*co*-NASI) (**A**−**E**), plus the homopolymer p(VBP) (**H**) as a control sample, were treated with a solution of TFEA. The amino group of the TFEA can react with the NHS−ester groups, and the fluorine groups can be easily detected by XPS. This model reaction is established as a reactivity assay whether proteins can be bound to the surface or not.[29,45] Table 5 summarizes the XPS atomic percentages for the TFEA-modified polymer films with TiO_2 substrate peaks subtracted, and the results were renormalized concentrations.

Fluorine was detected on all of the copolymer samples p(VBP-*co*-NASI) (**A**−**E**) after reaction with the TFEA. The amount of fluorine detected increased with increasing NHS content of the polymers. No fluorine was detected on the p(VBP) (**H**) coated control. The concentration of attached fluorine is lower than expected for a complete reaction of all NHS groups within the polymer. However, not all NHS groups present in the polymer may be accessible at the surface for reaction. These results show that the copolymer is able to bind molecules that have accessible primary amine groups.

Experiments to measure the coupling of BMP-2 to the copolymer films with ELISA are in progress.

Conclusions

With the aim of developing polymeric interlayers for binding bioactive proteins to implant surfaces, copolymers of VBP with NASI were synthesized and characterized. The copolymerization yields copolymers with an alternating sequence of the monomers, as evidenced by the *r* parameters ($r_{VBP} = 0.16$ and $r_{NASI} = 0.13$). These copolymers were successfully immobilized to titanium, as evidenced by infrared spectroscopy, XPS, and ToF-SIMS measurements. IR measurements indicated the interaction of the phosphonate group with the substrate. XPS measurements further substantiate the formation of well-defined polymer films, the thickness of which depends on the concentration of phosphonic acid ester groups in the polymer. However, no conclusive statement regarding the binding mechanism of the polymers is possible from the XPS data. The bound copolymer films were able to immobilize TFEA, showing that some of the active ester groups in the bound films would be accessible for protein immobilization. Experiments to couple proteins to the copolymer coated surfaces are currently under way.

The here described approach to immobilize proteins to titanium implant materials would be easy and versatile. It involves a simple spin or dip coating from solution to bind the polymers to the implant material surface, allowing even complicated geometries to be easily coated. Directly after surface washing, the protein should attach with no additional modification steps required. Furthermore, the polymeric interlayers are not restricted to titanium surfaces. The phosphonic acid ester-containing polymers should also be able to attach to other materials such as tantalum,[41] aluminum,[42] zirconium,[43] or steel.[44]

Acknowledgment. The authors would like to thank Michael Klopschar for cutting and polishing the titanium substrates. Dan Graham and Chi-Ying Lee are thanked for the helpful discussions. This work was supported as a part of the SFB 599 ("Biomedical Engineering") by the Deutsche Forschungsgemeinschaft (DFG) and by the NIH (NIBIB) Grant EB-002027 to the National ESCA and Surface Analysis Center for Biomedical Problems (NESAC/BIO).

Supporting Information Available. Calculation of reactivity ratios for p(VBP-*co*-NASI), and PCA results of the positive-ion ToF-SIMS spectra of PC1. This material is available free of charge via the Internet at http://pubs.acs.org.

References and Notes

(1) Hoffmann, A.; Weich, H. A.; Gross, G.; Hillmann, G. *Appl. Microbiol. Biotechnol.* **2001**, *57*, 294−308.
(2) Sykaras, N.; Iacopino, A. M.; Triplett, R. G.; Marker, V. A. *Clin. Oral Invest.* **2004**, *8*, 196−205.
(3) Gao, T.; Kousinioris, N.; Winn, S. R.; Wozney, J. M.; Uludag, R. *Materialwiss. Werkstofftech.* **2001**, *32*, 953−961.
(4) Zhu, H.; Wu, Q.; Shentu, J.; Wang, H.; Hu, Y.; Zhu, K.; Liu, J. *J. Bioact. Compat. Polym.* **2005**, *20*, 271−278.
(5) Hollinger, J. O.; Schmitt, J. M.; Buck, D. C.; Shannon, R.; Joh, S.-P.; Zegzula, H. D.; Wozney, J. *J. Biomed. Mater. Res.* **1998**, *43B*, 356−364.
(6) Noshi, T.; Yoshikawa, T.; Dohi, Y.; Ikeuchi, M.; Horiuchi, K.; Ichijima, K.; Sugimura, M.; Yonemasu, K.; Ohgushi, H. *Artif. Organs* **2001**, *25*, 201−208.
(7) Patel, M. P.; Pavlovic, P.; Hughes, F. J.; King, G. N.; Cruchley, A.; Braden, M. *Biomaterials* **2001**, *22*, 2081−2086.
(8) Gao, T.; Uludag, H. *J. Biomed. Mater. Res.* **2001**, *57A*, 92−100.
(9) Jennissen, H. P.; Zumbrink, T.; Chatzinikolaidou, M.; Stepphuhn, J. *Materialwiss. Werkstofftech.* **1999**, *30*, 838−845.
(10) Puelo, D. A.; Kissling, R. A.; Sheu, M.-S. *Biomaterials* **2002**, *23*, 2079−2087.
(11) Voggenreiter, G.; Hartl, K.; Assenmacher, S.; Chatzinikolaidou, M.; Rumpf, H. M.; Jennissen, H. P. *Materialwiss. Werkstofftech.* **2001**, *32*, 942−948.
(12) Karageorgiou, V.; Meinel, L.; Hofmann, S.; Malhotra, A.; Volloch, V.; Kaplan, D. *J. Biomed. Mater. Res.* **2004**, *71A*, 528−537.
(13) Xiao, S.-J.; Textor, M.; Spencer, N. D. *Langmuir* **1998**, *14*, 5507−5516.
(14) Rezania, A.; Johnson, R.; Lefkow, A. R.; Healy, K. E. *Langmuir* **1999**, *15*, 6931−6939.
(15) Gawalt, E. S.; Avaltroni, M. J.; Danahy, M. P.; Silverman, B. M.; Hanson, E. L.; Midwood, K. S.; Schwarzbauer, J. E.; Schwartz, J. *Langmuir* **2003**, *19*, 200−204.
(16) Danahy, M. P.; Avaltroni, M. J.; Midwood, K. S.; Schwarzbauer, J. E.; J. Schwartz, *Langmuir* **2004**, *20*, 5333−5337.
(17) Adden, N.; Gamble, L. G.; Castner, D. G.; Hoffmann, A.; Gross, G.; Menzel, H. *Langmuir* **2006**, *22*, 8197−8204.
(18) Puelo, D. A. *J. Biomed. Mater. Res.* **1997**, *37*, 222−228.
(19) Marcinko, S.; Fadeev, A. Y. *Langmuir* **2004**, *20*, 2270−2273.
(20) Silverman, B. M.; Wieghaus, K. A.; Schwartz, J. *Langmuir* **2005**, *21*, 225−228.
(21) Tosatti, S.; De Paul, S. M.; Askendal, A.; VandeVondele, S.; Hubbell, J. A.; Tengvall, P.; Textor, M. *Biomaterials* **2003**, *24*, 4949−4958.
(22) Yang, H. J.; Cole, C.-A.; Monji, N.; Hoffman, A. S. *J. Polym. Sci., Part A: Polym. Chem.* **1990**, *28*, 219−226.
(23) Adden, N.; Hoffmann, A.; Gross, G.; Windhagen, H.; Thorey, F.; Menzel, H. *J. Biomater. Sci., Polym. Ed.*, submitted for publication, 2006.
(24) Guerrero, G.; Mutin, P. H.; Vioux, A. *Chem. Mater.* **2001**, *13*, 4367−4373.
(25) Armarego, W. L. F.; Perrin, D. D. *Purification of Laboratory Chemicals*, 4th ed.; Butterworth-Heinemann: Oxford, 1996.
(26) Boutevin, B.; Hamoui, B.; Parisi, J.-P.; Améduri, B. *Eur. Polym. J.* **1996**, *32*, 159−163.

(27) Yu, Z.; Zhu, W.-X.; Cabasso, I. *J. Polym. Sci., Part A: Polym. Chem.* **1990**, *28*, 227−230.
(28) Griep-Raming, N.; Karger, M.; Menzel, H. *Langmuir* **2004**, *20*, 11811−11814.
(29) Noiset, O.; Schneider, Y.-J.; Marchand-Brynaert, J. *J. Polym. Sci., Part A: Polym. Chem.* **1997**, *35*, 3779−3790.
(30) Wagner, M. S.; Castner, D. G. *Langmuir* **2001**, *17*, 4649−4660.
(31) Wold, S.; Esbensen, K.; Geladi, P. *Chemom. Intell. Lab. Syst.* **1987**, *2*, 37−52.
(32) Thomas, L. C. *Interpretation of the Infrared Spectra of Organophosphorus Compounds*; Heyden: London, 1974.
(33) Viornery, C.; Chevolot, Y.; Léonard, D.; Aronsson, B.-O.; Péchy, P.; Mathieu, H. J.; Descouts, P.; Grätzel, M. *Langmuir* **2002**, *18*, 2582−2589.
(34) Textor, M.; Sittig, C.; Frauchinger, V.; Tosatti, S.; Brunette, D. M.; In *Titanium in Medicine: Material Science, Surface Science, Engineering, Biological Responses and Medical Applications*; Springer-Verlag: Berlin, 2001; pp 171−230.
(35) Nanci, A.; Wuest, J. D.; Peru, L.; Brunet, P.; Sharma, V.; Zalzal, S.; McKee, M. D. *J. Biomed. Mater. Res.* **1998**, *40*, 324−335.
(36) Hermanson, G. T. *Bioconjugate Techniques*; Academic Press: San Diego, CA, 1996.
(37) Böcking, T.; James, M.; Coster, H. G. L.; Chilcott, T. C.; Barrow, K. D. *Langmuir* **2004**, *20*, 9227−9235.
(38) Voicu, R.; Boukherroub, R.; Bartzoka, V.; Ward, T.; Wojtyk, J. T. C.; Wayner, D. D. M. *Langmuir* **2004**, *20*, 11713−11720.
(39) Textor, M.; Ruiz, L.; Hofer, R.; Rossi, A.; Feldman, K.; Hähner, G.; Spencer, N. D. *Langmuir* **2000**, *16*, 3257−3271.
(40) Beamson, G.; Briggs, D. *High-Resolution XPS of Organic Polymers*; The Scienta ESCA300 Database; John Wiley and Sons: Chichester, U. K., 1992.
(41) Brovelli, D.; Hähner, G.; Ruiz, L.; Hofer, R.; Kraus, G.; Waldner, A.; Schlösser, J.; Oroszlan, P.; Ehrat, M.; Spencer, N. D. *Langmuir* **1999**, *15*, 4324−4327.
(42) Maege, I.; Jaehne, E.; Henke, A.; H.-J. Adler, P.; Bram, C.; Jung, C.; Stratmann, M. *Macromol. Symp.* **1997**, *126*, 7−24.
(43) Woodward, J. T.; Ulman, A.; Schwartz, D. K. *Langmuir* **1996**, *12*, 3626−3629.
(44) Van Alsten, J. G. *Langmuir* **1996**, *12*, 7605−7614.
(45) Wirsen, A.; Sun, H.; Emilsson, L.; Albertson, A.-C. *Biomacromolecules* **2005**, 6, 2281−2289.

BM060473J